

Paolo Boccazzi · Andrea Zanzotto · Nicolas Szita ·
Sanchita Bhattacharya · Klavs F. Jensen ·
Anthony J. Sinskey

Gene expression analysis of *Escherichia coli* grown in miniaturized bioreactor platforms for high-throughput analysis of growth and genomic data

Received: 25 January 2005 / Revised: 9 March 2005 / Accepted: 12 March 2005 / Published online: 9 April 2005
© Springer-Verlag 2005

Abstract Combining high-throughput growth physiology and global gene expression data analysis is of significant value for integrating metabolism and genomics. We compared global gene expression using 500 ng of total RNA from *Escherichia coli* cultures grown in rich or defined minimal media in a miniaturized 50- μ l bioreactor. The microbioreactor was fabricated out of poly(dimethylsiloxane) (PDMS) and glass and equipped to provide on-line, optical measurements. cDNA labeling for microarray hybridizations was performed with the GeniconRLS system. From these experiments, we found that the expression of 232 genes increased significantly in cells grown in minimum medium, including genes involved in amino acid biosynthesis and central metabolism. The expression of 275 genes was significantly elevated in cells grown in rich medium, including genes involved in the translational and motility apparatuses. In general, these changes in gene expression levels were similar to those observed in 1,000-fold larger cultures. The increasing rate at which complete genomic sequences of microorganisms are becoming available offers an unprecedented opportunity for investigating these organisms. Our results from microscale cultures using just 500 ng of total RNA indicate that high-throughput integration of growth physiology and genomics will be possible with novel biochemical platforms and improved detection technologies.

Introduction

Global gene expression analysis using DNA microarrays is a technique widely applied in general biological research and in specialized fields such as drug screening, environmental testing, and clinical diagnosis (Debouck and Goodfellow 1999; Bodrossy and Sessitsch 2004). The ability to combine global gene expression analysis and high-throughput screening of microbial growth parameters allows the simultaneous rapid characterization of microbial strains at the physiological and molecular levels. The increasing availability of complete genomic sequences of microorganisms offers the unprecedented opportunity for detailed investigations of the functioning of these organisms. Genomic expression assays provide the ability to look at a single aspect of physiology and to see the interaction of those genes and operons with every other aspect of physiology.

To reach the goal of a rapid and informative high-throughput screening technology there remain two significant obstacles: first, as the techniques for DNA microarrays continue to be developed, an ongoing need persists for methods of performing microarrays on very small samples of bacterial cultures, and second, of the many metabolic and genetic experiments that can now be designed and performed in bacteria, only a small fraction can be tested using standard culture systems. The number of culture conditions that can be tested using tubes, flasks, and bench-scale bioreactors (with volumes of 0.5–10.0 l) is limited by the time required to obtain sufficient data, the effort required to obtain reproducible data, and the high costs of operation. In microbiological research, there clearly exists a need for a biochemical platform with integrated sensors yielding real-time data on process parameters. This allows high-throughput, parallel, and automated processing of a variety of microbial cultures under a variety of controlled conditions. Multidisciplinary efforts that link engineering and biology are generating novel miniaturized bioreactor platform devices that enable the production of multiple disposable bioreactor units for high-throughput data analysis (Kostov et al. 2001; Lamping et al. 2003; Maharbiz

P. Boccazzi (✉) · A. J. Sinskey
Department of Biology and Health Sciences and Technology,
Massachusetts Institute of Technology,
Cambridge, MA 02139, USA
e-mail: boccazzi@mit.edu
Tel.: +1-617-2535106
Fax: +1-617-2538550

A. Zanzotto · N. Szita · K. F. Jensen
Department of Chemical Engineering,
Massachusetts Institute of Technology,
Cambridge, MA 02139, USA

S. Bhattacharya
BioMicro Center, Department of Biology,
Massachusetts Institute of Technology,
Cambridge, MA 02139, USA

et al. 2004; Zanzotto et al. 2004). The 50- μ l bioreactor platform, recently described by Zanzotto et al. (2004), is a step toward a system that can be economically scalable and can generate real-time data for optical density (OD), pH, and dissolved oxygen (DO), thereby offering the advantages of high-throughput processes in terms of labor, time, reproducibility, and cost.

We demonstrated (Zanzotto et al. 2004) that *Escherichia coli* cultures grown in the 50- μ l microbioreactor platform exhibit reproducible growth characteristics in complex and minimal media, including OD, pH, and DO time-courses, as well as cell number and morphology, substrate uptake, and organic acid production. In these respects, growth of *E. coli* mimics that seen in conventional culture conditions (e.g. shake-flasks). They also demonstrated that serial harvest of microbioreactors was a feasible way to obtain samples for off-line analysis. The microbioreactor was fabricated out of poly(dimethylsiloxane) (PDMS) and glass, using soft lithography and was equipped with on-line measurements for OD, pH, and DO. Aeration of cultures was through a gas-permeable PDMS membrane.

In the present study, we sought to determine whether our microbioreactor format can be used to study global gene expression using DNA microarrays, as a step toward integrating high-throughput transcription profiling and bacterial fermentation analysis. To perform DNA microarray analysis for gene expression profiling, we used resonance light scattering (RLS) labeling technology. While microarray analysis is now well established, the technology continues to evolve, particularly toward an ongoing need for more sensitive methods and amplification techniques (Loge et al. 2002; Call et al. 2003). Current protocols for prokaryotic DNA microarrays require 5–10 μ g of total RNA as starting material. Bao et al. (2002) reported the high-sensitivity detection of DNA hybridization on microarrays of human genes using RLS technology, by labeling the cDNA with colloidal metal particles (40–120 nm diam.), which scatter light. As detailed by Yguerabide and Yguerabide (2001), the light-emitting power of a single RLS particle label is an order of magnitude greater than fluorescent labels such as Cy3 and Cy5. More recently, Francois et al. (2003) were able to detect and identify bacterial pathogens with the RLS system from small culture volumes, starting with only 10–500 ng of total RNA. We performed global gene expression analysis using 500 ng of total RNA from *E. coli* cultures grown in LB medium and in defined minimal medium in the 50- μ l bioreactor, using the GeniconRLS system (Invitrogen) for cDNA labeling. The data compare favorably with similar microarray studies conducted on bacterial cultures grown at larger scales. Our growth conditions were chosen based upon two earlier studies which compared gene expression in *E. coli* grown in 50-ml volumes of the same media (Tao et al. 1999; Wei et al. 2001), and their findings can be used to validate our experiments.

Materials and methods

Organism and growth conditions

E. coli FB21591 (*thiC*::Tn5-pKD46, Kan), obtained from the *E. coli* Genome Project at the University of Wisconsin (<http://www.genome.wisc.edu>), was used in all experiments. Cultures were grown in LB medium or defined minimal medium (DM), both supplemented with 10 g/l glucose. The composition of LB was: 10 g/l tryptone (Difco Laboratories, Sparks, Md.), 5 g/l yeast extract (Difco), 5 g/l NaCl. Following sterilization, the medium was supplemented with final concentrations of 10 g/l glucose (Mallinckrodt, Phillipsburg, N.J.), 100 mM MES buffer (pH 6.9; Sigma, St. Louis, Mo.), and 100 μ g/ml kanamycin (Sigma). The 40% (w/v) glucose stock was autoclaved for 20 min at 120°C, 150 kPa; and the MES (2 M) and kanamycin (100 mg/ml) stocks were filter-sterilized. The composition of the DM was: 60 mM K_2HPO_4 , 35 mM NaH_2PO_4 , 15 mM $(NH_4)_2SO_4$, 70 mM NH_4Cl , 0.8 mM $MgSO_4 \cdot 7H_2O$, 0.06 mM $Ca(NO_3)_2 \cdot 4H_2O$, 20 mM $FeCl_3$, 0.003 μ M $(NH_4)_6Mo_7O_{24} \cdot 4H_2O$, 0.4 μ M H_3BO_3 , 0.01 μ M $CuSO_4 \cdot 5H_2O$, 0.08 μ M $MnCl_2 \cdot 4H_2O$, 0.01 μ M $ZnSO_4 \cdot 7H_2O$, 10 g/l glucose, 100 μ M thiamine, 100 mM MES (pH 6.9), 100 μ g/ml kanamycin. Glucose, MES, and kanamycin were added to DM as stock solutions, as described for the LB medium. Thiamine was also added as stock solution (100 mM, previously filter-sterilized).

For inoculum preparation, the strain was first adapted to LB or DM as follows: 5 ml of LB were inoculated with a single colony from an overnight LB-kanamycin agar plate and incubated at 37°C on a roller drum at 60 rpm. At an OD_{600} of 1.0 ± 0.1 , 1.6 ml were used to inoculate 30 ml of fresh LB or DM in 500 ml baffled shake-flasks and incubated at 37°C on a horizontal rotary shaker at 150–200 rpm until the OD_{600} reached about 1.0. At this point, the culture was diluted in fresh LB or DM to reach an OD_{600} of about 0.05 and used to inoculate the microbioreactors.

Microbioreactor fermentations

Microbioreactors (Fig. 1) fabricated from PDMS and glass (Zanzotto et al. 2004) were utilized for all fermentations. A separate microbioreactor was fabricated for each experiment. The bottom layer in which the sensors were embedded, the body of the fermentor, and the aeration membrane were made of PDMS. The base support of the bioreactor was made of glass, which provided the necessary rigidity and the optical access. The working volume of the microbioreactor was 50 μ l. Optical sensing methods were selected to monitor OD, DO, and pH. The bottom layer of the microbioreactor contained two sensor foils (PreSens, Regensburg, Germany), one for DO and one for pH. The OD_{600} was used to monitor biomass. Light from an orange LED (L600-10 V, 600 nm; Epitex, Kyoto, Japan) was

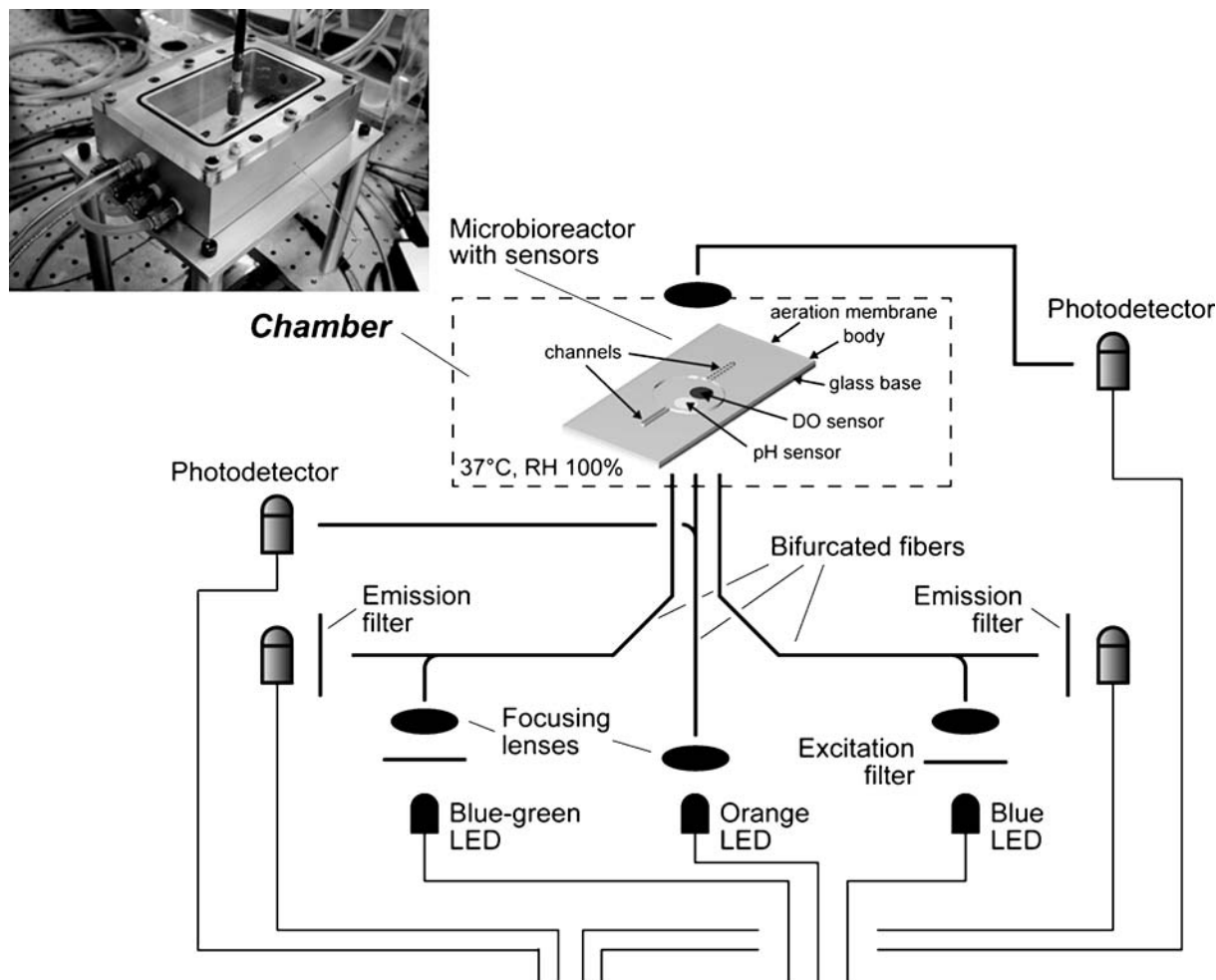


Fig. 1 Schematic of the microfermentor and experimental set-up. After inoculation, a single microbioreactor is placed inside the chamber, which is kept at 100% humidity and 37°C. Three optical fibers carry three different wavelengths of light to the bottom of the

microbioreactor for the three measurements: OD, DO, and pH. Photodetectors collect the transmitted or emitted light and send it to a lock-in amplifier, where the signal is detected and analyzed

passed through the microbioreactor, collected by a collimating lens (F230 SMA-A; Thorlabs, Newton, N.J.), and sent to a photodetector (PDA55; Thorlabs). The OD_{600} was calculated using Eq. 1.

$$OD = 33.33 \log_{10} \left(\frac{I_{\text{reference}}}{I_{\text{signal}}} \right) \quad ((1))$$

In Eq. 1, I_{signal} is the intensity of the signal and $I_{\text{reference}}$ is the intensity of the first measurement for a given experiment. The multiplication factor of 33.33 in Eq. 1 is used to normalize the data for the microbioreactor pathlength (300 μm), which enables direct comparisons with results from conventional cuvettes with pathlengths of 1 cm. This adjustment is only strictly valid if the absorption and light scattering by the cell culture are in a linear range. A calibration of OD measurements in the microbioreactor was performed using serial dilutions of an *E. coli* culture grown to an OD_{600} of about 7.0. The OD_{600} measurements of diluted cultures were made in the microbioreactor to a depth of 300 μm , using a Spectronic 20 Genesys spectrophotom-

eter (Spectronic Instruments, Rochester, N.Y.). The calibration data (Fig. 2) produced a linear fit with a slope close to 1.0.

All instruments were PC-controlled under a LabVIEW software routine (National Instruments, Austin, Tex.), which allowed for automated and on-line measurements of OD_{600} , pH, and DO every 10 min.

Each fermentation data set was obtained from an independent fermentation derived from a single colony inoculum and run in a single microbioreactor.

Experiments were carried out in an airtight, aluminum chamber (Fig. 1), which allowed control of humidity and the composition of the gas above the microbioreactor membrane; it also provided a large thermal mass, which stabilized the temperature at the desired set-point of 37°C. Temperature was controlled by circulating water at 37°C through the chamber base. In addition to controlling environmental parameters, the chamber provided optical isolation and optical access from directly above and below the microbioreactor.

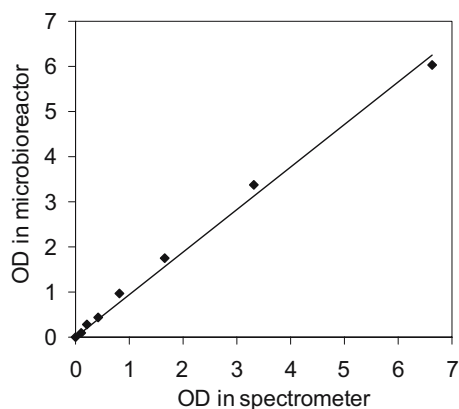


Fig. 2 Calibration curve for OD measurements in the microbio-reactors. A dilution series of *E. coli* cells was used to compare direct measurements in a spectrometer with pathlength-adjusted measurements in the microbio-reactor. The OD was measured at 600 nm in both systems; and the OD in the microbio-reactor was adjusted to a pathlength of 1 cm (from 300 μm)

The microbio-reactor was inoculated from outside of the chamber by injection with a 1-ml syringe, equipped with a 23 gauge needle, through the microbio-reactor side-channels (Fig. 1). The needle holes created in the channels were then sealed with epoxy and the microbio-reactor secured to the base of the chamber. Open reservoirs of water were placed inside the chamber to provide humidity. Maintaining high humidity within the chamber minimized evaporation loss through the PDMS membrane. The chamber was then closed and real-time data collection initiated. Sterility was maintained through the addition of the antibiotic kanamycin to the growth medium. Additional details of the microbio-reactor and its set-up are described by Zanzotto et al. (2004).

Total RNA isolation

Total RNA was isolated from three independent 50- μl fermentations in LB and three in DM. To isolate total RNA from 50- μl cultures, we developed the following procedure. Cells were harvested during exponential growth at $\text{OD}_{600} \sim 1.0$, typically at a population density of $2\text{--}4 \times 10^9$ cells/ml; and thus $\sim 1\text{--}2 \times 10^8$ cells were recovered from 50 μl . To harvest cultures, the incubation chamber was opened and the entire culture withdrawn from the microbio-reactor through the PDMS membrane, using a 200- μl Pipetman. The samples were transferred immediately to 1.5-ml Eppendorf tubes containing 2 vol. of RNAlprotect Bacteria (Qiagen, Valencia, Calif.) for RNA stabilization. After 5 min of incubation at room temperature, cells were pelleted and resuspended in 200 μl of TE (10 mM Tris-HCl, 1 mM EDTA, pH 8.0) containing lysozyme (15 mg/ml) and incubated for 20 min at room temperature on a Nutator (Becton Dickinson, Parsippany, N.J.) for gentle mixing. The samples were then transferred to 2-ml tubes (Sarstedt, Newton, N.C.) containing 50 mg of acid-washed zirconia/silica beads (0.1 mm diam.; Biospec Products, Bartlesville, Okla.) and lysed in a FastPrep FP120 beadbeater (Qbiogene, Carlsbad, Calif.) for 90 s at maximum speed. We

found that we obtained consistently higher yields and better RNA quality when we performed a combination of enzymatic and mechanical cell disruption. Total RNA isolation was performed using an RNeasy kit (Qiagen) by loading the lysed sample, without the beads, directly onto RNeasy columns and then following the manufacturer's protocol. The concentration and quality of the purified RNA was assessed by determination of the OD ratio at 260 nm/280 nm and analysis using an Agilent 2100 Bioanalyzer (Palo Alto, Calif.). RNA samples were stored at -80°C . The average yield of total RNA from 50 μl of *E. coli* culture grown in LB or DM to an OD_{600} of about 1.0 was approximately 3 μg and 1 μg , respectively.

Microarray hybridizations and analysis

DNA microarrays were printed at the MIT BioMicro Center (Cambridge, Mass.) with a BioRobotics MicroGrid Two printer (Genomic Solutions, Ann Arbor, Mich.) on Corning GAPS slides (Acton, Mass.) with a 50-mers oligo set (MWG-Biotech, High Point, N.C.) composed of 4,288 gene-specific oligonucleotide probes representing the complete *E. coli* (K12) genome.

Microarray hybridizations were performed with the GeniconRLS two-color array detection system (Invitrogen, Carlsbad, Calif.), based on RLS technology. From each fermentation, 500 ng of total RNA were used to generate cDNA labeled with biotin-16-dUTP (Enzo Life Sciences, Framingham, N.Y.) for LB samples and fluorescein-12-dUTP (Roche, Indianapolis, Ind.) for DM samples. Direct labeling was performed with the LabelStar kit (Qiagen), using a modified protocol as follows. For each of the biotin-labeled reactions, the labeling mix contained the following components: 5 μl of $10\times$ buffer, 5 μl dNTP-Mix H, 1 μl of biotin-labeled dUTP, 1 μl of random DNA hexamers (Roche Diagnostic, Indianapolis, Ind.), 0.5 μl of RNase inhibitor, 2.5 μl of LabelStar reverse transcriptase, 15 μl of RNase-free water, and 20 μl of denatured RNA template. The fluorescein-labeled mixes were prepared as described for the biotin-labeled mixes, except that 2 μl of fluorescein-labeled dUTP and 14 μl of RNase-free water were used. dNTP mixes contained dATP, dCTP, dGTP (0.5 mM each), and 0.04 mM dTTP. RNA templates were denatured before cDNA labeling by adding 2 μl of denaturation solution to 18 μl of RNA sample, followed by incubation for 5 min at 65°C in a water bath and subsequent cooling on ice.

Labeling mixes were incubated for 2 h at 37°C in a thermocycler with a hot lid. Then, 1 μl of dTTP (20 mM) was added to each labeling mix and incubation at 37°C was continued for 1 h. Reactions were then stopped with the addition of 2 μl of stop solution LS (Invitrogen). Purification of labeled cDNA was performed immediately, using the LabelStar kit (Qiagen) as directed, except that each of the six samples was purified independently. Also, in the final step of the purification, each column was eluted twice with 50 μl of EB (Qiagen). Each labeled cDNA sample (100 μl) was then diluted with 400 μl of RNase-free water. One labeled cDNA sample generated

from a LB culture and one labeled cDNA sample generated from a DM culture were pooled and concentrated to 12 μ l with a Microcon Y-30 0.5-ml column (Millipore, Bedford, Mass.) as directed by the manufacturer.

Before hybridization, microarray slides were baked in an oven at 80°C for 2 h. After cooling, the slides were cross-linked with UV light in a Stratalinker 2400 (Stratagene, La Jolla, Calif.) at 300 mJ. Slide prehybridization was performed as recommended by the manufacturer: incubated for 30 min at 42°C in a polypropylene slide mailer filled with 25 ml of pre-hybridization solution, washed twice in deionized water at room temperature, and dried with a stream of filtered nitrogen gas.

We performed three co-hybridizations, in each case comparing LB and DM fermentations on a single array (Fig. 4). The hybridization mixes (25 μ l) contained 12.5 μ l of hybridization solution (pre-heated to 42°C), 0.5 μ l of hybridization blocker (salmon sperm DNA, 10 mg/ml), and 12 μ l of labeled target cDNA (biotin-, fluorescein-labeled cDNA). We used a smaller volume than the one recommended in the protocol, since we used lifter slips (Eric Scientific, Portsmouth, N.H.) of smaller dimensions (24 \times 24 mm). Hybridization mixes were incubated at 95°C for 5 min. Before hybridization, the lifter slips were washed first with deionized water, then with 70% ethanol, and finally dried with a stream of filtered nitrogen gas. The lifter slips were then placed over the arrays and the hot (95°C) hybridization mix was added to one of the free edges of the lifter slip, to flood the array area by capillary action. The slides were placed in ArrayIt hybridization cassettes (TeleChem International, Sunnyvale, Calif.), together with 250 μ l of water for humidity control, and placed in a 42°C incubator overnight. Post-hybridization washes were performed as directed. Microarray slides were then blocked in 25 ml of blocking solution (Invitrogen) for 2 min at room temperature. The slides were then placed on a wet paper towel and placed in a Tupperware container, which functioned as a hydration chamber. Each array was covered with 45 μ l of the RLS particle mix, composed of 15 μ l of Anti-Biotin RLS particle Au (gold), 15 μ l of AntiFluorescein particle Ag (silver), and 15 μ l RLS particle diluent. Lifter slips were washed and dried as described above and carefully lowered over the array area. Microarray slides were then incubated in the hydration chamber for 1 h. The RLS particle wash was performed as directed with wash solutions, using a squirt bottle and a slide mailer. Following final washes in a glass tank with deionized water, the slides were dried with a stream of filtered nitrogen gas and archived in 25 ml of archiving solution (Invitrogen) and dried for about 2 h in a laminar flow hood.

To determine spot intensities, microarray slides were scanned in a GSD-501 RLS detection and imaging instrument (Invitrogen) and image data were calculated using MolecularWare software (Cambridge, Mass.).

To obtain normalized ratios from the two fluorescence intensity channels, we performed rank-invariant intensity-dependent non-linear normalization LOWESS (Tseng et al. 2001) on the intensity data of each array, using the lcDNA ver. 0.03 program (Hyduke et al. 2003). Normalized in-

Table 1 Pearson's correlation coefficients among the three microarray replicates

	Array 1	Array 2	Array 3
Array 1	1.0000	0.8156	0.8231
Array 2	0.8156	1.0000	0.8234
Array 3	0.8231	0.8234	1.0000

tensity ratios were calculated, using DM as numerator and LB as denominator. The two growth conditions were compared by determining mean log₂ intensity ratios across the three replicates. Genes were considered upregulated if the log₂ ratio of DM intensity (positive numbers) over LB intensity (negative numbers) for each ORF was greater than +1 or less than -1. The complete set of gene expression data can be viewed on the NCBI gene expression omnibus web site (<http://www.ncbi.nlm.nih.gov/geo/>, accession number GSE1981). Pearson's correlation coefficients were calculated using the three normalized log ratios to determine the concordance among the microarrays (Table 1).

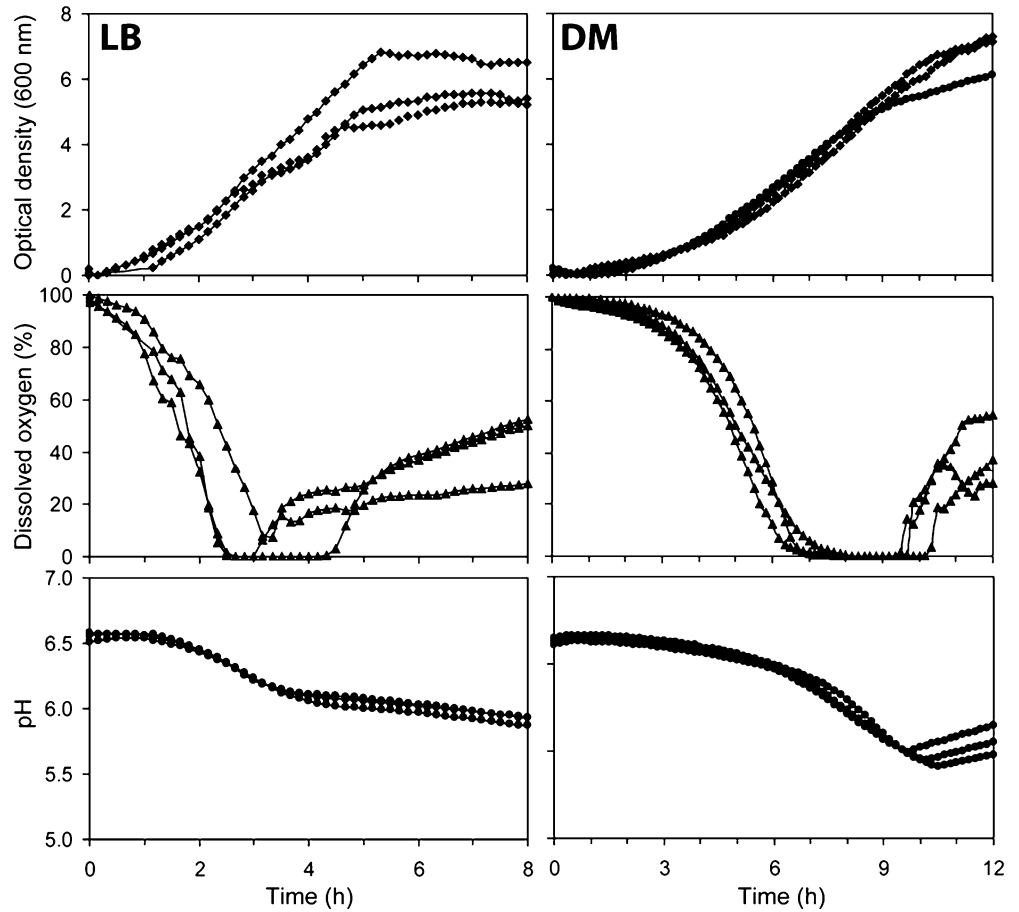
For gene annotation, *E. coli* sequences were compared to proteins in the cluster of orthologous group (COG) database (Tatusov et al. 1997) using the BlastP sequence similarity search program (Altschul et al. 1997). Assignment to a particular COG group was made by transferring the COG function of the top alignment to the *E. coli* protein. This allowed a high-throughput annotation of gene functions.

Results

Triplicate fermentations of *E. coli* grown in LB and DM in 50- μ l microbioreactors with on-line measurements for OD₆₀₀, pH, and DO are shown in Fig. 3. All fermentations were independent (inoculum derived from a single colony) and run in single microbioreactors on different days. As expected (Cooper 1991), in the microbioreactors *E. coli* grew faster in rich than in minimal medium, with average generation times of 28.8 \pm 3.2 min and 45.3 \pm 2.1 min in LB and DM, respectively. Also as expected, oxygen depletion and acidification of the medium occurred earlier in LB cultures than in DM cultures, since growth was more rapid in rich medium. Growth patterns across the three fermentations in each medium were reproducible. To investigate global gene expression in cells grown in our miniaturized 50- μ l bioreactors, we carried out triplicate fermentations in DM and LB. Cells for RNA isolation were harvested when the cultures reached an OD₆₀₀ of about 1.0. At this population density, the average pH of both media was about pH 6.6 and the DO concentrations were on average 60–80% in DM and 40–60% in LB, where 100% was the oxygen concentration of saturated medium in equilibrium with air.

To assess gene expression profiles under the two growth conditions, we identified upregulated genes by taking the log₂ ratio of the spot mean intensities of DM over LB (Fig. 4). The Pearson's correlation coefficient among the three microarrays replicates was about 0.82 for all three

Fig. 3 Fermentations ($n=3$) of *E. coli* grown in 50- μ l micro-bioreactors in LB (left panels) and in DM (right panels). The fermentations, each represented by a single data set, were performed on different days in single micro-bioreactors



arrays (Table 1). Table 2 summarizes the numbers of up-regulated genes under the two growth conditions, annotated by functional group and class. The total number of up-regulated genes in the two media was 507, of which 232 were up-regulated in DM and 275 in LB (Table 2). When *E. coli* was grown in DM, a larger number of “Metabolism” genes was up-regulated, while in LB more “Cellular processes” and “Information storage and processing” genes were up-regulated.

These results were expected, since *E. coli* growing on glucose (DM) as sole carbon and energy source must generate de novo building blocks (i.e. amino acids, vitamins, nucleosides, etc.) for macromolecular synthesis. But *E. coli* grows more rapidly in LB, since the building blocks for macromolecular synthesis are provided by yeast extract and tryptone, and both transcription and translation are expected to be up-regulated (Gaal et al. 1997).

Fig. 4 *E. coli* microarrays (left) hybridized with cDNA obtained from 500 ng of total RNA from cultures grown in 50- μ l micro-bioreactors in DM (green) and LB (red). Normalized mean spot intensities averaged from three replicates from each of the two growth conditions were plotted against each other (right); and the log₂ ratios of DM (green) over LB (red) intensities were binned to identify genes up-regulated more than two-fold

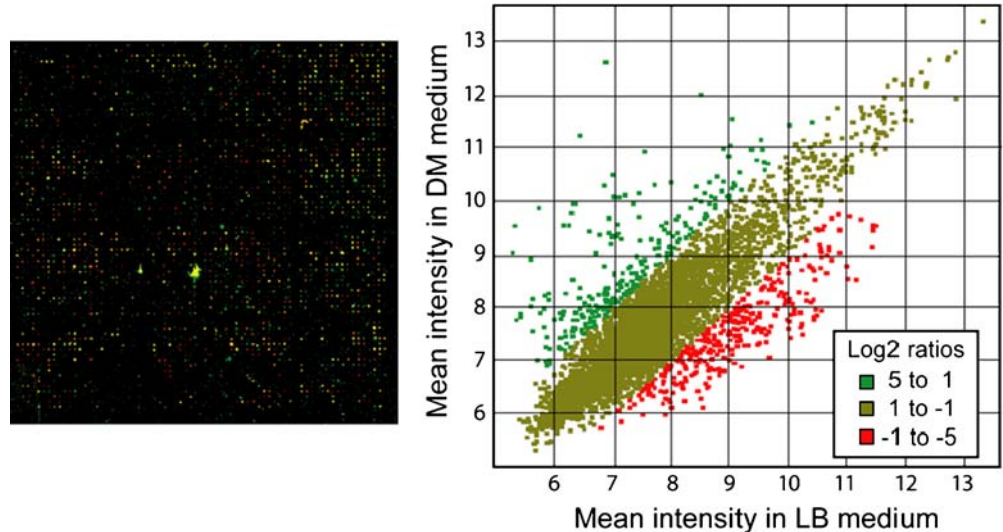


Table 2 Numbers of upregulated genes in *E. coli* growing in DM and LB. Functional annotation was performed by comparing *E. coli* sequences to proteins in the COG database

Function group	Function class	Medium	
		DM	LB
Metabolism	Amino acid transport and metabolism	48	10
	Carbohydrate transport and metabolism	19	20
	Coenzyme metabolism	2	4
	Energy production and conversion	25	6
	Lipid metabolism	–	4
	Nucleic acid transport and metabolism	2	5
	Cellular processes	Cell division and chromosome partitioning	–
Cell envelope biogenesis, outer membrane		7	7
Cell motility and secretion		1	16
Defense mechanisms		–	3
Inorganic ion transport and metabolism		13	13
Posttranslational modification, protein turnover		5	3
Signal transduction mechanisms		5	5
Information storage and processing		DNA replication, recombination, and repair	8
	Transcription	11	22
	Translation, ribosomal structure, and biogenesis	2	3
	Poorly characterized	84	143
Total	232	275	

The total number of upregulated genes in the “Metabolism” functional group, in *E. coli* grown in DM versus LB was 96 and 49 respectively (Table 3). The major differences arose in the two functional classes “Amino acid transport and metabolism” and “Energy production and conversion”. Specifically, in DM, 48 “Amino acid transport and metabolism” genes were upregulated, including genes involved in the synthesis of all 20 amino acids found in proteins (Table 3). For example, three genes for proline biosynthesis (*proVWX*) were strongly upregulated, with *proX* showing the most significant increase in this functional class. Other genes highly upregulated in DM were *leuB* (responsible, with *leuACD*, for leucine biosynthesis), the three genes of the *thrABC* operon for threonine biosynthesis, four genes (*aroCFGL*) for the synthesis of chorismate (a central intermediate in aromatic amino acids biosynthesis), and seven genes (*cysACDHJMP*) for the synthesis and metabolism of cysteine.

In LB medium, only ten genes in the functional class “Amino acid transport and metabolism” were upregulated, none of which are involved in amino acid biosynthesis but

Table 3 Differential expression profile of genes involved in metabolism in *E. coli* grown in DM and LB. Genes were considered upregulated if the log₂ ratio of DM intensity (positive numbers) over LB intensity (negative numbers) for each ORF was greater than +1 or less than –1

Gene ID	Gene product	Log ₂ intensity ratio (DM/LB)
	Amino acid transport and metabolism	
<i>proX</i>	Transport system for glycine and proline	5.8
<i>leuB</i>	3-Isopropylmalate dehydrogenase	4.2
<i>thrB</i>	Homoserine kinase	3.6
<i>proV</i>	Transport system for glycine, betaine and proline	3.5
<i>oppA</i>	Oligopeptide transport; periplasmic binding protein	3.4
<i>dppA</i>	Dipeptide transport protein	3.3
<i>leuC</i>	3-Isopropylmalate isomerase (dehydratase)	3.1
<i>metE</i>	Tetrahydropteroyltriglutamate methyltransferase	3.1
<i>gltD</i>	Glutamate synthase, small subunit	2.9
<i>asd</i>	Aspartate-semialdehyde dehydrogenase	2.9
<i>ddpA</i>	Putative hemin-binding lipoprotein	2.4
<i>thrC</i>	Threonine synthase	2.3
<i>gltB</i>	Glutamate synthase, large subunit	2.3
<i>hisC</i>	Histidinol-phosphate aminotransferase	2.3
<i>livJ</i>	High-affinity amino acid transport system	2.2
<i>gadB</i>	Glutamate decarboxylase isozymes	2.2
<i>proW</i>	Transport system for glycine and proline	2.1
<i>trpC_1</i>	N-(5-Phosphoribosyl)anthranilate isomerase	1.8
<i>cysM</i>	Cysteine synthase B, O-acetylserine sulfhydrylase B	1.7
<i>cysD</i>	ATP:sulfurylase, subunit 2	1.6
<i>trpC_1</i>	N-(5-Phosphoribosyl)anthranilate isomerase	1.5
<i>ygjI</i>	Putative oxidoreductase	1.4
<i>aroL</i>	Shikimate kinase II	1.4
<i>hisF</i>	Imidazole glycerol phosphate synthase subunit	1.4
<i>hisI_1</i>	Phosphoribosyl-amp cyclohydrolase	1.4

Table 3 (continued)

Gene ID	Gene product	Log2 intensity ratio (DM/LB)
<i>yhfX</i>	Predicted amino acid racemase	-1.2
<i>tdcB</i>	Threonine dehydratase, catabolic	-1.2
<i>ptrB</i>	Protease II	-1.2
<i>sdaB</i>	L-Serine dehydratase (deaminase), L-SD2	-1.0
Coenzyme metabolism		
<i>folE</i>	GTP cyclohydrolase I	1.5
<i>bioD</i>	Dethiobiotin synthetase	1.4
<i>abgT</i>	Putative pump protein (transport)	-1.8
<i>ubiA</i>	4-Hydroxybenzoate-octaprenyltransferase	-1.5
<i>ubiX</i>	3-Octaprenyl-4-hydroxybenzoate carboxy-lyase	-1.5
<i>moaA</i>	Molybdopterin biosynthesis, protein A	-1.1
Nucleic acid transport and metabolism (F)		
<i>cmk</i>	Cytidylate kinase	2.1
<i>purF</i>	Amidophosphoribosyl-transferase	1.2
<i>guaA</i>	GMP synthetase (glutamine-hydrolyzing)	-2.0
<i>dgt</i>	Deoxyguanosine triphosphate triphosphohydrolase	-1.5
<i>purH</i>	Phosphoribosylcarboxamide-formyltransferase	-1.1
<i>guaB</i>	IMP dehydrogenase	-1.1
<i>pyrI</i>	Aspartate carbamoyltransferase, regulatory subunit	-1.1
Lipid metabolism		
<i>atoE</i>	Short-chain fatty acid transporter	-2.6
<i>ynjF</i>	Putative cytochrome oxidase	-2.4
<i>idnO</i>	5-Keto-D-gluconate 5-reductase	-1.2
<i>entA</i>	2,3-Dihydro-2,3-dihydroxybenzoate dehydrogenase	-1.2
Carbohydrate transport and metabolism		
<i>gata</i>	Galactitol-specific of phosphotransferase system	4.2
<i>gatZ</i>	Putative tagatose 6-phosphate kinase 1	3.5
<i>gatY</i>	Tagatose-bisphosphate aldolase 1	3.0
<i>gapC</i>	Glyceraldehyde 3-phosphate dehydrogenase C	2.6
<i>yicM</i>	Putative transport protein	2.5

Table 3 (continued)

Gene ID	Gene product	Log2 intensity ratio (DM/LB)
<i>leuD</i>	Isopropylmalate isomerase subunit	1.4
<i>gatD</i>	Galactitol-1-phosphate dehydrogenase	1.4
<i>ddpF</i>	ATP-binding component of a transport system	1.4
<i>ilvN</i>	Acetolactate synthase I, valine sensitive	1.3
<i>cysH</i>	3'-Phosphoadenosine 5'-phosphosulfate reductase	1.3
<i>thrA</i>	Aspartokinase I, homoserine dehydrogenase I	1.3
<i>livG</i>	ATP-binding component of amino acid transport system	1.2
<i>serA</i>	D-3-Phosphoglycerate dehydrogenase	1.2
<i>aroC</i>	Chorismate synthase	1.2
<i>ilvD</i>	Dihydroxyacid dehydratase	1.1
<i>trpB</i>	Tryptophan synthase, beta protein	1.1
<i>aroG</i>	Arabinoheptulosonate-7-phosphate synthase	1.1
<i>aroF</i>	Arabinoheptulosonate-7-phosphate synthase	1.1
<i>cysA</i>	Sulfate permease A protein	1.1
<i>aegA_2</i>	Putative oxidoreductase, Fe-S subunit	1.1
<i>glnH</i>	Periplasmic glutamine-binding protein; permease	1.1
<i>speE</i>	Spermidine synthase	1.0
<i>yfcK_2</i>	Putative peptidase	1.0
<i>phnC</i>	ATP-binding component of phosphonate transport	1.0
<i>ilvB</i>	Acetolactate synthase I, valine-sensitive	1.0
<i>leuA</i>	2-Isopropylmalate synthase	1.0
<i>poxB</i>	Pyruvate oxidase	1.0
<i>ygfK</i>	Putative oxidoreductase, Fe-S subunit	1.0
<i>xasA</i>	Acid sensitivity protein, putative transporter	-2.3
<i>tnaA</i>	Tryptophanase	-2.0
<i>gltK</i>	Glutamate/aspartate transport system permease	-1.8
<i>ydgR</i>	Putative transport protein	-1.7
<i>yhaP</i>	Putative L-serine dehydratase	-1.6
<i>potH</i>	Putrescine transport protein; permease	-1.4

Table 3 (continued)

Gene ID	Gene product	Log2 intensity ratio (DM/LB)
<i>galP</i>	Galactose-proton symport of transport system	-1.1
<i>malG</i>	Part of maltose permease, inner membrane	-1.1
<i>gmhA</i>	Phosphoheptose isomerase	-1.0
<i>lacY</i>	Galactoside permease (M protein)	-1.0
Energy production and conversation		
<i>aceB</i>	Malate synthase A	4.8
<i>aceA</i>	Isocitrate lyase	3.5
<i>yodB</i>	Putative cytochrome	2.6
<i>sucC</i>	Succinyl-CoA synthetase, beta subunit	2.4
<i>narJ</i>	Nitrate reductase 1, delta subunit	2.3
<i>narG</i>	Nitrate reductase 1, alpha subunit	2.0
<i>sdhA</i>	Succinate dehydrogenase, flavoprotein subunit	1.7
<i>nuoB</i>	NADH dehydrogenase I chain B	1.6
<i>pntA</i>	Pyridine nucleotide transhydrogenase, alpha subunit	1.5
<i>nuoE</i>	NADH dehydrogenase I chain E	1.5
<i>sdhA</i>	Succinate dehydrogenase, flavoprotein subunit	1.3
<i>fdx</i>	[2FE-2S] ferredoxin, electron carrer protein	1.3
<i>nuoG</i>	NADH dehydrogenase I chain G	1.3
<i>ybiC</i>	Putative dehydrogenase	1.3
<i>hyfI</i>	Hydrogenase 4 Fe-S subunit	1.2
<i>glcB</i>	Malate synthase G	1.2
<i>fdhD</i>	Affects formate dehydrogenase-N	1.2
<i>nuoI</i>	NADH dehydrogenase I chain I	1.2
<i>gltA</i>	Citrate synthase	1.2
<i>sucD</i>	Succinyl-CoA synthetase, alpha subunit	1.2
<i>hyfF</i>	Hydrogenase 4 membrane subunit	1.2
<i>prpC</i>	Putative citrate synthase; propionate metabolism	1.2
<i>nuoH</i>	NADH dehydrogenase I chain H	1.1
<i>sdhD</i>	Succinate dehydrogenase, hydrophobic subunit	1.1

Table 3 (continued)

Gene ID	Gene product	Log2 intensity ratio (DM/LB)
<i>gapC_2</i>	Glyceraldehyde 3-phosphate dehydrogenase	2.4
<i>gatY</i>	Tagatose-bisphosphate aldolase 1	1.9
<i>otsA</i>	Trehalose-6-phosphate synthase	1.8
<i>rbsB</i>	D-ribose periplasmic binding protein	1.7
<i>pykF</i>	Pyruvate kinase I (formerly F), fructose stimulated	1.5
<i>gatC</i>	PTS system galactitol-specific enzyme IIC	1.4
<i>glgX</i>	Part of glycogen operon, glycosyl hydrolase	1.4
<i>glgC</i>	Glucose-1-phosphate adenylyltransferase	1.3
<i>uxaC</i>	Uronate isomerase	1.3
<i>ptxA</i>	Putative PTS system enzyme II A component	1.3
<i>alsC</i>	Putative transport system permease protein	1.3
<i>malK</i>	Transport system for maltose	1.1
<i>ycjR</i>	Putative transient receptor potential locus	1.1
<i>talA</i>	Transaldolase A	1.0
<i>agaD</i>	PTS system, <i>N</i> -acetylglucosamine enzyme IID	-2.6
<i>xapB</i>	Xanthosine permease	-2.2
<i>shiA</i>	Putative transport protein, shikimate	-2.0
<i>uidB</i>	Glucuronide permease	-1.7
<i>frvX</i>	Frv operon protein	-1.7
<i>agaW</i>	PTS system <i>N</i> -acetylglactosamine-specific IIC	-1.7
<i>mglC</i>	Methyl-galactoside transport and galactose taxis	-1.6
<i>ptsG</i>	PTS system, glucose-specific IIBC component	-1.5
<i>rhaT</i>	Rhamnose transport	-1.4
<i>ybhC</i>	Putative pectinesterase	-1.3
<i>agaC</i>	PTS system <i>N</i> -acetylglactosamine-specific IIC	-1.3
<i>yfeV_2</i>	Putative PTS enzyme II	-1.3
<i>fucl</i>	L-fucose isomerase	-1.3
<i>ebgA</i>	Evolved beta-D-galactosidase, gene	-1.2
<i>gntP</i>	Gluconate transport system permease 3	-1.2
<i>xyle</i>	Xylose-proton symport	-1.2

Table 3 (continued)

Gene ID	Gene product	Log2 intensity ratio (DM/LB)
<i>ydgN</i>	Putative membrane protein	1.0
<i>ybiW</i>	Putative formate acetyltransferase	-1.6
<i>ydeP</i>	Putative oxidoreductase, major subunit	-1.4
<i>lldP</i>	L-lactate permease	-1.3
<i>cydA</i>	Cytochrome d terminal oxidase, polypeptide subunit I	-1.1
<i>araB</i>	L-ribulokinase	-1.1
<i>hyfD</i>	Hydrogenase 4 membrane subunit	-1.0

four of which are involved in amino acid degradation: *sdaB* and *yhaP* (glycine), *tnaA* (tryptophan) and *tdcB* (threonine).

In the functional classes “Carbohydrate transport and metabolism” and “Energy production and conversion”, again a larger number of genes was upregulated in DM than in LB (Table 3). In DM cultures, genes involved in acetate utilization and the glyoxylate shunt (*aceA*, *aceB*, *gltA*), those in the tricarboxylic acid cycle, [e.g. citrate synthetase (*sdhAD*), succinyl-CoA synthetase (*sucCD*), and the NADH dehydrogenase genes (*nuoBEGHI*) involved in oxidative phosphorylation and ubiquinone biosynthesis were upregulated. Also upregulated were genes and operons involved in galactitol and tagatose transport and metabolism (*gatACDYZ*) and in glycolysis, such as glyceraldehyde 3-phosphate dehydrogenase (*gapC 1*) and pyruvate kinase (*pykF*).

During growth in LB, the most strongly upregulated genes belonging to the two functional classes “Carbohydrate transport and metabolism” and “Energy production and conversion” were those involved in the expression of the phosphotransferase system (PTS) protein *N*-acetyl glucosamine (*agaCDW*) and another PTS protein that is glucose-specific (*ptsG*).

In contrast, compared with growth in DM, the *E. coli* cells grown in LB had a larger number of genes categorized as “Cellular processes” that were upregulated (Table 2). The marked differences within this functional group were in the functional class “Cell motility and secretion”, where *E. coli* grown in LB exhibited 17 upregulated genes (Table 4), with eight of these involved in flagellum assembly (*fliACNS*, *flgACEK*) and five involved in chemotaxis (*cheAYZ*, *tar*, *motB*), indicating that the strain grown in rich medium at an OD of 1.0, was actively motile.

As expected, higher expression of genes from the group “Information storage and processing” was observed in LB than in DM (35 vs 21; Table 2). Indeed, *E. coli* divides more rapidly in LB than in DM and faster-growing cultures synthesize protein at a higher rate than the slower-growing ones (Grunberg-Manago 1996; Keener and Nomura 1996; Gaal et al. 1997). Of the 35 “Information” genes upregulated in LB medium, most (22) belonged to the “Transcrip-

Table 4 Differential expression profile of genes involved in cellular processes in *E. coli* grown in DM and LB

Gene ID	Gene product	Log2 ratio (DM/LB)
Cell envelope biogenesis, outer membrane		
<i>yedS</i>	Putative outer membrane protein	2.5
<i>dniR</i>	Transcriptional regulator for nitrite reductase	2.4
<i>spr</i>	Putative lipoprotein	1.6
<i>murG</i>	UDP- <i>N</i> -acetylglucosamine	1.2
<i>nlpD</i>	Lipoprotein	1.1
<i>b1980</i>	ADP-heptose:LPS heptosyltransferase	1.1
<i>yaiP</i>	Polysaccharide metabolism	-2.1
<i>rhcC</i>	Protein in <i>rhc</i> element	-1.7
<i>mreD</i>	Rod shape-determining protein	-1.7
<i>rhcE</i>	RhcE protein in <i>rhc</i> element	-1.6
<i>rfbC</i>	dTDP-6-deoxy-D-glucose-3,5 epimerase	-1.3
<i>kdsB</i>	CTP: CMP-3-D-manno- octulosonate transferase	-1.1
Cell motility and secretion		
<i>flhA</i>	Flagellar biosynthesis	2.0
<i>fliC</i>	Flagellar biosynthesis; flagellin	-2.5
<i>tar</i>	Methyl-accepting chemotaxis protein II	-2.2
<i>motB</i>	Enables flagellar motor rotation	-2.1
<i>yqiH</i>	P pilus assembly protein, chaperone PapD	-1.6
<i>ycbT</i>	Homologue of <i>Salmonella</i> FimH protein	-1.5
<i>fliA</i>	Flagellar biosynthesis	-1.4
<i>cheA</i>	Sensory transducer kinase	-1.4
<i>ppdD</i>	Prelipin peptidase dependent protein	-1.4
<i>flgE</i>	Flagellar biosynthesis, hook protein	-1.3
<i>cheZ</i>	Chemotactic response; CheY protein phosphatase	-1.2
<i>fliN</i>	Flagellar biosynthesis, component of motor switch	-1.2
<i>yehD</i>	P pilus assembly protein, pilin FimA	-1.2
<i>fliS</i>	Flagellar biosynthesis; repressor of (RflA activity)	-1.2
<i>flgA</i>	Flagellar biosynthesis; periplasmic P ring	-1.1
<i>flgC</i>	Flagellar biosynthesis, basal-body rod	-1.1

Table 4 (continued)

Gene ID	Gene product	Log2 ratio (DM/LB)
<i>flgK</i>	Flagellar biosynthesis, hook-filament	-1.1
<i>cheY</i>	Chemotaxis regulator	-1.0
Signal transduction mechanisms		
<i>glnL</i>	Histidine protein kinase sensor for GlnG regulator	1.6
<i>ybcZ</i>	Putative 2-component sensor protein	1.4
<i>ypdA</i>	Putative sensor protein	1.2
<i>phoQ</i>	Sensor protein PhoQ	1.2
<i>ygeV</i>	Putative transcriptional Regulator	1.2
<i>yjiY</i>	Putative carbon starvation protein	-2.1
<i>ybdQ</i>	Universal stress protein UspA	-1.6
<i>yeiL</i>	cAMP-binding proteins-catabolite gene activator	-1.3
<i>fimZ</i>	Fimbrial Z protein; probable signal transducer	-1.1
<i>barA</i>	Sensor-regulator, activates OmpR by phosphorylation	-1.0
Cell division and chromosome partitioning		
<i>sulA</i>	Suppressor of <i>lon</i> ; inhibits cell division	-1.0
Defense mechanisms		
<i>bacA</i>	Bacitracin resistance	-1.9
<i>mcrC</i>	Component of McrBC restriction system	-1.1
<i>dinF</i>	DNA-damage-inducible protein F	-1.0
Inorganic ion transport and metabolism		
<i>cysJ</i>	Sulfite reductase (NADPH)	1.6
<i>oppB</i>	Oligopeptide transport permease protein	1.6
<i>dps</i>	Global regulator, starvation conditions	1.5
<i>oppC</i>	Homologue of <i>Salmonella</i> transport permease	1.4
<i>cutCm</i>	Copper homeostasis protein	1.4
<i>yejE</i>	Putative transport system permease protein	1.4
<i>cysC</i>	Adenosine 5'-phosphosulfate kinase	1.3
<i>cysP</i>	Thiosulfate-binding protein	1.3
<i>phnM</i>	Phosphonate metabolism	1.2
<i>cysWm</i>	Sulfate transport system permease W protein	1.2

Table 4 (continued)

Gene ID	Gene product	Log2 ratio (DM/LB)
<i>yoaE_2</i>	Putative transport protein	1.1
<i>nikB</i>	Transport of nickel, membrane protein	-2.0
<i>focB</i>	Probable formate transporter (formate channel 2)	-1.8
<i>nikC</i>	Transport of nickel, membrane protein	-1.8
<i>kdpB</i>	ATPase of high-affinity potassium transport system	-1.7
<i>yliD</i>	Putative transport system permease protein	-1.7
<i>nirCm</i>	Nitrite reductase activity	-1.5
<i>tolQ</i>	Inner membrane protein, membrane-spanning	-1.5
<i>dppB</i>	Dipeptide transport system permease protein 1	-1.5
<i>yliC</i>	Putative transport system permease protein	-1.3
<i>emrE</i>	Methylviologen resistance	-1.3
<i>ccmD</i>	Heme exporter protein C	-1.2
<i>yieL</i>	Putative xylanase	-1.1
<i>fecB</i>	Citrate-dependent iron transport	-1.1
<i>znuA</i>	Putative adhesin	1.1
<i>ybhI</i>	Putative membrane pump protein	1.1
Posttranslational modification, protein turnover		
<i>slpA</i>	FKBX-type peptidyl-prolyl cis-trans isomerase	1.5
<i>nrdH</i>	Glutaredoxin-like protein; hydrogen donor	1.5
<i>hslJ</i>	Heat-shock protein HslJ	1.4
<i>grxB</i>	Glutaredoxin 2	1.1
<i>ybeW</i>	Putative dnaK protein	1.0
<i>sirA</i>	Regulator of disulfide bond formation	-1.3
<i>groL</i>	GroEL, chaperone Hsp60, heat-shock protein	-1.2
<i>yqjG</i>	Putative transferase	-1.0

tion" functional class (Table 2). Among the more strongly expressed were *hcaR* (Table 5), a transcriptional regulator of the LysR family that controls the *hca* cluster for propionate catabolism (Diaz et al. 1998), and *iclR*, a repressor of the *aceBA* operon that mediates acetate utilization. Accordingly, the *aceBA* genes were strongly upregulated in *E. coli* grown in DM (Table 3).

In DM, *rpoS*, which encodes the RNA polymerase sigma subunit regulating many cellular responses to environmental stress (Hengge-Aronis 1993; Loewen and Hengge-Aronis 1994), was strongly expressed (Table 5),

Table 5 Differential expression profile of genes involved in information storage and processing in *E. coli* grown in DM and LB

Gene ID	Gene product	Log2 ratio (DM/LB)
Transcription		
<i>cspG</i>	Homologue of <i>Salmonella</i> cold shock protein	3.5
<i>feaR</i>	Regulatory protein for 2-phenylethylamine catabolism	2.4
b1770	Putative DEOR-type transcriptional regulator	2.1
<i>rpoS</i>	RNA polymerase, sigma S (sigma38) factor	1.7
<i>yrbL</i>	ORF, hypothetical protein	1.6
<i>cspH</i>	Cold-shock-like protein; cold-shock protein	1.6
<i>dsdC</i>	D-Serine dehydratase transcriptional activator	1.5
<i>nusA</i>	Transcription pausing; L factor	1.5
<i>rnc</i>	RNase III, ds RNA	1.4
<i>narP</i>	Nitrate/nitrite response regulator (sensor NarQ)	1.3
<i>torR</i>	Response transcriptional regulator for torA	1.2
<i>ygeV</i>	Putative transcriptional regulator	1.2
<i>uhpA</i>	Positive activator of <i>uhpT</i> transcription	1.1
<i>psiF</i>	Induced by phosphate starvation	1.1
<i>ygeP</i>	ORF, hypothetical protein	1.1
<i>ygRi</i>	ORF, hypothetical protein	1.0
<i>ylcA</i>	Putative 2-component transcriptional regulator	1.0
<i>hcaR</i>	Transcriptional activator of <i>hca</i> cluster	-2.6
<i>ygiU</i>	Transcription regulator containing HTH domain	-2.1
<i>ydeO</i>	Putative ARAC-type regulatory protein	-1.8
<i>yghW</i>	Transcription regulator containing HTH domain	-1.8
<i>ypdB</i>	Putative 2-component transcriptional regulator	-1.7
<i>cadC</i>	Transcriptional activator of cad operon	-1.7
<i>yqeI</i>	Putative sensory transducer	-1.6
<i>ygZi</i>	Transcription regulator containing HTH domain	-1.6
<i>ydiP</i>	Putative ARAC-type regulatory protein	-1.6
<i>iclR</i>	Repressor of <i>aceBA</i> operon	-1.6

Table 5 (continued)

Gene ID	Gene product	Log2 ratio (DM/LB)
<i>ybaD</i>	Predicted transcriptional regulator	-1.5
<i>yjcT</i>	Putative NAGC-like transcriptional regulator	-1.5
<i>fliA</i>	Flagellar biosynthesis	-1.4
b2635	Predicted transmembrane transcriptional regulator	-1.4
<i>hcaR-r</i>	Transcriptional activator of <i>hca</i> cluster	-1.4
<i>perR</i>	Putative transcriptional regulator LYSR-type	-1.3
<i>yhcO</i>	Barstar, RNase (barnase) inhibitor	-1.3
<i>nhaR</i>	Transcriptional activator of <i>nhaA</i>	-1.3
gntRR	Regulator of gluconate (<i>gnt</i>) operon	-1.2
<i>viaG</i>	Predicted transcriptional regulator	-1.2
<i>ykgD</i>	Putative ARAC-type regulatory protein	-1.2
<i>ycjW</i>	Putative LACI-type transcriptional regulator	-1.2
<i>pssR</i>	Regulator of <i>pssA</i>	-1.2
<i>fimZ</i>	Fimbrial Z protein; probable signal transducer	-1.1
<i>paaX</i>	Phenylacetic acid-responsive transcriptional repressor	-1.1
<i>ygjJ</i>	Transcription regulator containing HTH domain	-1.1
<i>yegW</i>	Putative transcriptional regulator	-1.1
<i>lexA</i>	Regulator for SOS(<i>lexA</i>) regulon	-1.0
<i>rhaR</i>	Positive regulator for <i>rhaRS</i> operon	-1.0
<i>nusG</i>	Component in transcription antitermination	-1.0
DNA replication, recombination, and repair		
<i>yi91b</i>	IS911 hypothetical protein (IS911B)	1.9
<i>trs5_1</i>	IS5 transposases	1.4
<i>ycaJ</i>	Putative polynucleotide enzyme	1.3
<i>dinJ</i>	Damage-inducible protein J	1.2
<i>recR</i>	Recombination and repair	1.2
<i>rnhB</i>	RNase HII, degrades RNA of DNA-RNA hybrids	1.1
<i>dnaX</i>	DNA polymerase III, tau and gamma subunits	1.1

Table 5 (continued)

Gene ID	Gene product	Log2 ratio (DM/LB)
<i>dnaQ</i>	DNA polymerase III, epsilon subunit	1.1
b0105	Transposase and inactivated derivatives	-2.5
<i>fimB</i>	Regulator for fimA	-2.2
b2596	Transposase and inactivated derivatives	-2.0
b1788	Transposase	-1.9
<i>lit</i>	Phage T4 late gene expression	-1.8
<i>ynjG</i>	ORF, hypothetical protein	-1.7
<i>intA</i>	Prophage CP4-57 integrase	-1.6
<i>sbmC</i>	SbmC protein	-1.6
<i>nfi</i>	Endonuclease V (deoxyinosine 3'endoduclease)	-1.5
b0309	Transposase and inactivated derivatives	-1.4
b1903	Transposase	-1.4
b2191	Transposase and inactivated derivatives	-1.4
<i>alkB</i>	DNA repair system specific for alkylated DNA	-1.2
<i>hupB-r</i>	DNA-binding protein HU-beta, NS1 (HU-1)	-1.2
<i>recG</i>	DNA helicase, resolution of Holliday junctions	-1.2
<i>recN</i>	Protein used in recombination and DNA repair	-1.1
b0165	Transposase and inactivated derivatives	-1.1
<i>recA</i>	DNA strand exchange and renaturation	-1.1
<i>ycfH</i>	Mg-dependent DNase	-1.0
<i>seqA</i>	Negative modulator of initiation of replication	-1.0
Translation, ribosomal structure and biogenesis		
<i>tsf</i>	Protein chain elongation factor EF-Ts	1.4
<i>rsuA</i>	16S pseudouridylate 516 synthase	1.1
<i>smpA</i>	Small membrane protein A	-1.6
<i>lysU</i>	Lysine tRNA synthetase; heat shock protein	-1.5
<i>rplS</i>	50S ribosomal subunit protein L19	-1.1

in agreement with the reports of Tao et al. (1999) and Wei et al. (2001), and suggests that RpoS regulation may be important not only during the transition between the exponential and stationary phases, but also in the early and late logarithmic phases. Other genes that exhibited upregulation in DM were *narP*, a nitrate/nitrite response regulator belonging to the LuxR/UhpA family of the two-component regulatory system controlling the expression of several genes involved in anaerobic fermentation and respiration (Rabin and Stewart 1993), and *uhpA* of the two-component regulatory system UhpB/UhpA, involved in the uptake of hexose phosphates (Dahl et al. 1997).

Discussion

Rapid screening for microorganisms exhibiting specific patterns of gene expression and protein production is critical for progress in microbiology, biotechnology, and the pharmaceutical industry. We used a novel microbioreactor platform that is scalable and has the advantage of providing real-time data on bacterial growth parameters for OD₆₀₀, pH, and DO. *E. coli* cultures grown in this microbioreactor platform exhibited growth patterns that are comparable with those from bench-scale 500-ml bioreactors (Zanzotto et al. 2004). Microbioreactors have the potential to provide much of the data and functionality that a large bioreactor system does, while offering the advantages of scale for high-throughput processes. Also, the use of microbioreactors is of increasing value, since recent advances in molecular biology make it possible to create large numbers of evolved biocatalysts, new pathway designs, and to discover a variety of unique biological organisms from diverse sources. It is likely that microbioreactors with integrated sensors and actuators will be the driving force behind research in high-throughput screening for general biological research.

Our aim was to demonstrate that the microbioreactor platform we had previously described (Zanzotto et al. 2004) can be used not only to grow potentially large numbers of microbial strains to study their physiology, but also to link this real-time information to global gene expression analysis. To this end, we performed a microarray analysis on 500 ng of total RNA from *E. coli* cultures grown in LB medium and in minimal medium (DM) in an instrumented 50- μ l bioreactor, using the RLS system for cDNA labeling. Two previous studies (Tao et al. 1999; Wei et al. 2001) reported microarray analysis on *E. coli* MG1655 grown in rich and minimal media in 50-ml batch culture in 250-ml Erlenmeyer flasks. The two studies then used different methods for microarray analysis. Tao et al. (1999) used 1 μ g of total RNA (with 32P-dCTP to label cDNA) and Nylon DNA arrays; and Wei et al. (2001) used 6 μ g of total RNA, Cy3 and Cy5 fluorophores to label cDNA, and printed microarrays with PCR-amplified ORFs.

The two studies reached similar general conclusions indicating that, in *E. coli* grown in minimal medium, metabolic genes for processes such as amino acid biosynthesis

and energy production and conversion are upregulated, while in cultures grown in rich medium, genes involved in translation and ribosome structure and biogenesis are stimulated. These results confirm general predictions that bacteria grown in minimal media must generate the monomers needed to build macromolecules de novo, whereas in conditions that support rapid growth they increase the assemblage of ribosomes and translation factors de novo.

In our miniaturized system, we found that *E. coli* grown in minimal medium, with glucose as sole carbon and energy source, upregulated a large number of genes involved in amino acid biosynthesis, energy production, and energy conversion. This parallels the two large-scale studies described above, in which threonine, phenylalanine, leucine, serine, tryptophan, isoleucine/valine, and histidine biosynthesis genes were over-expressed. Other similarities included the overexpression of *aceAB*, involved in acetate metabolism, and *rpoS*, a global gene expression regulator. Several additional genes that were upregulated in minimal medium in our microbio-reactors were also upregulated in minimal medium in at least one of the two studies mentioned.

However, we found some differences with reported results (Tao et al. 1999; Wei et al. 2001) in the gene expression profiles of *E. coli* cultures grown in LB. One was the clear upregulation of genes for chemotaxis and motility in our system. Our result was, however, expected since *E. coli* is motile in LB but not in minimal medium due to catabolite repression by glucose (sole carbon source) in the medium (Silverman and Simon 1974). Also in our study, we did not observe large differences between cells grown in LB versus DM in their expression of the genes for translational apparatus, ribosomal structure, and biogenesis. This dissimilarity with previous reports may be attributable to differences in growth and analytical conditions, such as medium composition, phase of physiological growth at which cells were harvested, type of microarray platform used, etc. It could also be due to the cDNA labeling system that we used. At the time of our investigations, the RLS system had proven to be sufficiently sensitive to obtain gene expression profiles of human genes (Bao et al. 2002) and we were among the first to apply it to bacterial cultures. In a more recent study, the RLS system was used to efficiently detect bacterial cultures down to 10^5 cells (Francois et al. 2003). In our experiments with RLS, we found some variability between replicates. Also, we were not able to confirm all of our results in dye-swap experiments (data not shown) and excluded these data from the analysis. We believe that these difficulties may be due to the facts that: (1) we were using much more complex arrays than Francois et al. (2003), who tested a limited number of ORFs and used a single RLS label (gold), and (2) the RLS system may require optimization to perform a global gene expression analysis. Nevertheless, it was useful in our proof of concept study of cDNA arrays from small volume bacterial cultures.

In summary, we have shown that microbio-reactors can be used to reproducibly grow bacterial cultures, we have developed protocols to isolate high-quality total RNA from small volumes of cultures grown in microbio-reactors, and

we have performed differential gene expression analysis in *E. coli* grown under two different conditions in microbio-reactors equipped with real-time monitoring of growth parameters. In general, *E. coli* exhibited gene expression profiles that were predicted for growth under the conditions tested, essentially in agreement with data from 1,000-fold larger culture volumes.

The ability to obtain reliable data from 50- μ l cultures demonstrates that, in the future, rapid screening of metabolic and genomic data will be possible with the use of scalable microbio-reactor platforms and improvements in technology that increase the sensitivity of microarrays.

Acknowledgements We gratefully acknowledge the DuPont-MIT Alliance (DMA) for funding. The authors are also grateful to Dr. Jefferson Parker for his help with gene annotation, Dr. Phil Lessard for continuous, stimulating discussions and for reviewing the manuscript, and Prof. Jacqueline Piret for critically reviewing the manuscript.

References

- Altschul SF, Madden TL, Schaffer AA, Zhang J, Zhang Z, Miller W, Lipman DJ (1997) Gapped BLAST and PSI-BLAST: a new generation of protein database search programs. *Nucleic Acids Res* 25:3389–3402
- Bao P, Frutos AG, Greef C, Lahiri J, Muller U, Peterson TC, Warden L, Xie XY (2002) High-sensitivity detection of DNA hybridization on microarrays using resonance light scattering. *Anal Chem* 74:1792–1797
- Bodrossy L, Sessitsch A (2004) Oligonucleotide microarrays in microbial diagnostics. *Curr Opin Microbiol* 7:245–254
- Call DR, Borucki MK, Loge FJ (2003) Detection of bacterial pathogens in environmental samples using DNA microarrays. *J Microbiol Methods* 53:235–243
- Cooper S (1991) Synthesis of the cell surface during the division cycle of rod-shaped, gram-negative bacteria. *Microbiol Rev* 55:649–674
- Dahl JL, Wei BY, Kadner RJ (1997) Protein phosphorylation affects binding of the *Escherichia coli* transcription activator UhpA to the *uhpT* promoter. *J Biol Chem* 272:1910–1919
- Debouck C, Goodfellow PN (1999) DNA microarrays in drug discovery and development. *Nat Genet* 21:48–50
- Diaz E, Ferrandez A, Garcia JL (1998) Characterization of the *hca* cluster encoding the dioxygenolytic pathway for initial catabolism of 3-phenylpropionic acid in *Escherichia coli* K-12. *J Bacteriol* 180:2915–2923
- Francois P, Bento M, Vaudaux P, Schrenzel J (2003) Comparison of fluorescence and resonance light scattering for highly sensitive microarray detection of bacterial pathogens. *J Microbiol Methods* 55:755–762
- Gaal T, Bartlett MS, Ross W, Turnbough CL Jr, Gourse RL (1997) Transcription regulation by initiating NTP concentration: rRNA synthesis in bacteria. *Science* 278:2092–2097
- Grunberg-Manago M (1996) Regulation of the expression of aminoacyl-tRNA synthetases and translation factors. In: Neidhardt FC, Curtis III R, Ingraham JL, Lin ECC, Low KB, Magasanik B, Reznikoff WS, Riley M, Schaechter M, Umberger HE (eds) *Escherichia coli* and *Salmonella typhimurium*: cellular and molecular biology. ASM, Washington, D.C., pp 1432–1457
- Hengge-Aronis R (1993) Survival of hunger and stress: the role of *rpoS* in early stationary phase gene regulation in *E. coli*. *Cell* 72:165–168
- Hyduke DR, Rohlin L, Kao KC, Liao JC (2003) A software package for cDNA microarray data normalization and assessing confidence intervals. *Omics* 7:227–234

- Keener J, Nomura M (1996) Regulation of ribosome biosynthesis. In: Neidhardt FC III, Ingraham JL, Lin ECC, Low KB, Magasanik B, Reznikoff WS, Riley M, Schaechter M, Umbarger HE (eds) *Escherichia coli* and *Salmonella typhimurium*: cellular and molecular biology. ASM, Washington, D.C., pp 1417–1431
- Kostov Y, Harms P, Randers-Eichhorn L, Rao G (2001) Low-cost microbioreactor for high-throughput bioprocessing. *Biotechnol Bioeng* 72:346–352
- Lamping SR, Zhang H, Allen B, Shamlou PA (2003) Design of a prototype miniature bioreactor for high throughput automated bioprocessing. *Chem Eng Sci* 58:747–758
- Loewen PC, Hengge-Aronis R (1994) The role of the sigma factor sigma S (KatF) in bacterial global regulation. *Annu Rev Microbiol* 48:53–80
- Loge FJ, Thompson DE, Call DR (2002) PCR detection of specific pathogens in water: a risk-based analysis. *Environ Sci Technol* 36:2754–2759
- Maharbiz MM, Holtz WJ, Howe RT, Keasling JD (2004) Microbioreactor arrays with parametric control for high-throughput experimentation. *Biotechnol Bioeng* 85:376–381
- Rabin RS, Stewart V (1993) Dual response regulators (NarL and NarP) interact with dual sensors (NarX and NarQ) to control nitrate- and nitrite-regulated gene expression in *Escherichia coli* K-12. *J Bacteriol* 175:3259–3268
- Silverman M, Simon M (1974) Flagellar rotation and the mechanism of bacterial motility. *Nature* 249:73–74
- Tao H, Bausch C, Richmond C, Blattner FR, Conway T (1999) Functional genomics: expression analysis of *Escherichia coli* growing on minimal and rich media. *J Bacteriol* 181:6425–6440
- Tatusov RL, Koonin EV, Lipman DJ (1997) A genomic perspective on protein families. *Science* 278:631–637
- Tseng GC, Oh M-K, Rohlin L, Liao JC, Wong WH (2001) Issues in cDNA microarray analysis: quality filtering, channel normalization, models of variations and assessment of gene effects. *Nucleic Acids Res* 29:2549–2557
- Wei Y, Lee JM, Richmond C, Blattner FR, Rafalski JA, LaRossa RA (2001) High-density microarray-mediated gene expression profiling of *Escherichia coli*. *J Bacteriol* 183:545–556
- Yguerabide J, Yguerabide EE (2001) Resonance light scattering particles as ultrasensitive labels for detection of analytes in a wide range of applications. *J Cell Biochem S37*:71–81
- Zanzotto A, Szita N, Boccazzi P, Lessard P, Sinskey AJ, Jensen KF (2004) Membrane-aerated microbioreactor for high-throughput bioprocessing. *Biotechnol Bioeng* 87:243–254